EUROFUSION WPJET1-PR(16) 14476

E Joffrin et al.

Impact of divertor geometry on H-mode confinement in the JET metallic wall

Preprint of Paper to be submitted for publication in
Nuclear Fusion

This work has been carried out within the framework of the EUROfusion Consortium and has received funding from the Euratom research and training programme 2014-2018 under grant agreement No 633053. The views and opinions expressed herein do not necessarily reflect those of the European Commission.

Impact of divertor geometry on H-mode confinement in the JET metallic wall

E. Joffrin 1), P. Tamain 1), E. Belonohy 2), H. Bufferand 1), P. Buratti 3), C. Challis 4), E. Delabie 5), P. Drewelow 6), D. Dodt 6), L. Frassinetti 7), J. Garcia 1), C. Giroud 4), M. Groth 8), J. Hobirk 6), A. E. Jarvinen 8), H.-T. Kim 4) , F. Koechl 9), U. Kruezi 4), B. Lipschutz 10), P. Lomas 4), E. de la Luna 11), T. Loarer 1), P. Maget 1), C. Maggi 4), G. Matthews 4), F. Maviglia 3), A. Meigs 4), I. Nunes 12), G. Pucella 3), F. Rimini 4), S. Saarelma 4), E. Solano 11), A.C.C. Sips 2), M. Tsalas 13), I. Voitsekhovitch 4), H. Weisen 2), and the JET Contributors*

EUROfusion Consortium JET, Culham Science Centre, Abingdon, OX14 3DB, UK
1) IRFM, CEA, F-13108 Sant-Paul-lez-Durance, France.
2) JET Exploitation Unit, Culham science site, OX143DB Abingdon, Oxon, UK.
3) Unita Tecnica Fusione - ENEA, C.R. Frascati, Roma , Italy.
4) CCFE, Culham Science Centre, Abingdon, Oxon, OX14 3DB, UK
5) ERM, Ecole Royale Militaire Avenue de la Renaissance 30, 1000 Brussels, Belgium
6) Max-Planck-Institut fur Plasmaphysik, 85748, Garching Germany.
7) Royal Institute of Technology KTH, SE-10044 Stockholm, Sweden
8) Tekes, VTT, PO Box 1000, 02044 VTT, Finland.
9) ÖAW/ATI, Atominstitut, TU Wien, 1020 Vienna, Austria
10) York Plasma Institute, Department of Physics, University of York, York YO10 5DD, UK
11) Laboratorio Nacional de Fusión, CIEMAT, 28040 Madrid, Spain
12) Istituto de plasmas e fusao nuclear, Lisboa, Portugal
13) FOM institute DIFFER, Nieuwegein, Netherlands
E-mail contact of the main author: emmanuel.joffrin@cea.fr

Abstract:

Recent experiments with the ITER-like wall have demonstrated that changes in divertor strike point position are correlated with strong modification of the global energy confinement. The impact on energy confinement is observable both on the pedestal confinement and core normalised gradients. The corner configuration shows an increased core density gradient length and ion pressure indicating a better ion confinement. The study of neutral re-circulation indicates the neutral pressure in the main chamber varies inversely with the energy confinement and a correlation between the pedestal total pressure and the neutral pressure in the main chamber can be established. It does not appear that charge exchange losses nor momentum losses could

*See the Appendix of F. Romanelli et al., Proceedings of the 25th IAEA Fusion Energy Conference 2014, Saint Petersburg, Russia

explain this effect, but it may be that changes in edge electric potential are playing a role at the plasma edge. This study emphasizes the importance of the scrape-off layer (SOL) conditions on the pedestal and core confinement.

1- Introduction

The transition in JET from a fully carbon wall to the ITER-like wall (ILW) with tungsten (W) plasma facing components (PFCs) in the divertor and primarily beryllium PFCs in the main chamber has been an essential step in 2011 for demonstrating the compatibility of ITER scenario with a metallic environment [1]. The initial experiments have shown that the operational domain at H_{98y2}=1 is significantly reduced with the JET ITER-like wall (JET-ILW) mainly because of the need to inject large amount of gas (above 10^{22}D/s) to control core radiation mostly due to W. These first results have stressed the importance of the edge plasma and plasma-wall interaction physics in determining the core plasma performance [2]. The change of wall material has also modified the impurity mix and the recycling flux of the main gas and this could play a role in the physics of core and pedestal confinement. The importance of the particle source as a key control parameter is confirmed by the degradation of the core and pedestal confinement obtained when puffing gas in order to limit impurity accumulation in the plasma. Maximisation of confinement, control of metallic impurity sources and heat loads are the main challenges facing the further development of the ITER scenarios in JET.

For these reasons, specific exploration of the effect of divertor geometries on confinement have been conducted in JET in 2013 and 2014 to identify the divertor conditions leading to the optimum confinement and thermal neutron rate. This was explored for both the baseline (β_N=2) and hybrid scenario (β_N=3) with low shape magnetic configuration (δ=0.2) with the objective to investigate the possible influence of neutral recycling on the plasma confinement based on experimental analyses and modelling.

2- Experimental set-up and confinement observations

A series of type I ELMy H-mode discharges have been developed for JET with different divertor magnetic topology in order to isolate the effect of divertor recycling. The three equilibria/configurations have identical bulk plasma volume but the position of the strike-points is positioned differently with respect to the inner and outer pumping ducts. All three plasma shapes have a low upper triangularity (δ=0.2) so as to minimize recycling from the possible interaction of the plasma with the main chamber. Figure 1a shows the magnetic equilibria as reconstructed by EFIT [3]. The 3 cases will be referred to as the horizontal, corner and vertical

---

*See the Appendix of F. Romanelli et al., Proceedings of the 25th IAEA Fusion Energy Conference 2014, Saint Petersburg, Russia

targets in the remainder of this paper. With these three topologies, baseline scenario type [4] has been run with Ip=2.5MA and B_T=2.7T (q_{95}=3.2) at two different input power (15 and 23MW, i.e. β_N~1.5 and ~2) (fig 1b). In addition, hybrid scenario [5] with Ip=2.0MA and B_T=2.35T (q_{95}=3.8, β_N~3) has also been compared in the horizontal and corner configurations. In both scenario cases, different level of deuterium gas injection rate have been employed in the inner private flux region (see fig 1) only except for a few cases where the gas was injected from the main chamber at the outboard mid-plane for comparison. Also in the case of the baseline scenario, one of the two JET cryogenic pumps (pumping speed of ~50m^3/s each) has been switched off for a few discharges during the experiment in an attempt to separate the effect of neutral pumping and recycling on confinement.

It is observed (fig 2) that for identical fuelling rates, pumping and input power, the discharges on the horizontal and vertical target configurations have similar normalised confinement factor H_{98y2} ~0.7, while for the corner configuration a normalised confinement factor of 0.9 can be reached, close to the level of confinement for identical discharges with the carbon wall (JET-C). Several contributions in the past have reported that deuterium puffing (from the main chamber or the divertor) impacts negatively on the confinement for both the JET-C [6] and the JET-ILW [2]. In the present cases, it appears that the variation in divertor geometry and therefore in neutral recycling and pumping also impact confinements. This effect could be also observed in dedicated pulses in the JET-C as pointed out recently [5], but it is much stronger in the JET-ILW.

Although the hybrid scenario is not achieved yet in stationary conditions, the effect of the divertor geometry on the energy confinement is also observable. For low plasma shape, an increase of the normalised energy confinement factor by 10% when the strike points were moved to the corner of the divertor [5],. Given that the pedestal is playing a strong role in the observed improved confinement [7] this would suggest that pedestal confinement is affected by the change of divertor configuration.

Since the changes by the different divertor geometry have very small impact on the plasma bulk geometry (less than 2% in elongation κ and minor radius a which are included in the engineering parameters of the IPBy2 confinement scaling), the change in confinement resulting from the divertor geometry modifications cannot impact on the IPBy2 confinement scaling law [8] used as a reference here (plasma current, toroidal field and input power are kept identical otherwise). Note also that both horizontal target and corner have about the same line integrated density. The vertical target has on the other hand a lower line average density than the other two. This in principle should lead to an increase of the normalised confinement owing to the positive

*See the Appendix of F. Romanelli et al., Proceedings of the 25th IAEA Fusion Energy Conference 2014, Saint Petersburg, Russia

dependence of the IPB98y2 scaling with the line average density ($n^{0.4}$). Also, it should be noted that the distance of the separatrix to the main chamber wall does not vary significantly respect to the SOL width, excluding a large influence on the confinement.

As shown on figure 1a, the change in divertor geometry does also change the lower triangularity (δ_L=0.38 (horizontal) δ_L=0.31 (corner) δ_L=0.27 (vertical) to some extent (making a variation of the mean triangularity from 0.27 to 0.215). This modest variation of the lower triangularity by ~30% is not expected to play a major role on the observed confinement variation. As reported earlier in previous JET studies the lower triangularity is not playing a significant role on confinement [9]. We conclude, therefore that the edge and scrape-off (SOL) conditions (recycling neutral and/or pumping) are the dominant player in the confinement of these discharges.

3- Core and pedestal experimental analysis

The observed changes in energy confinement are consistent with the changes in core plasma density, temperature and pressure profiles (fig 3). The corner case is characterized by ion (from core charge exchange spectroscopy) and electron kinetic pressures (from the high resolution Thomson scattering: HRTS) substantially higher than the two other cases, the difference reaching almost 50% at the centre of the plasma. The higher measured neutron rate for the corner configuration is consistent with higher Ti for otherwise identical neutral source rate from the neutral beam power.

Interestingly, the gain in plasma pressure is achieved due to changes in either the core temperature or density profiles. The horizontal and corner configuration discharges present about the same density level, but the electron and ion temperatures are 50% larger in the corner case. On the contrary, the vertical configuration discharge exhibits much lower ELM averaged density than the other two (possibly because of increased pumping as measured by the higher neutral pressure in the pumping duct). However, the electron temperature is similar to that of the corner case and the ion temperature profile is intermediate between the horizontal and corner cases. This suggests that the mechanisms explaining the degradation of the confinement in the horizontal and vertical configurations with respect to the corner may not be identical transport wise.

Differences in the kinetic profiles are observed both on the pedestal pressure (Pe is 50% larger at the top of the pedestal in the corner configuration) and in the core gradients. For similar power heat flux the temperature gradient length R/L_{Te} (computed between r/a=0.3 and 0.7 using HRTS measurements) changes by less than 20% (fig 4) with the radial position of the outer strike point. On the other hand, the density gradient length R/L_n is 2 times larger in the corner

*See the Appendix of F. Romanelli et al., Proceedings of the 25th IAEA Fusion Energy Conference 2014, Saint Petersburg, Russia

configuration than on the horizontal target suggesting that the particle channel transport is the significantly affected. This change of density peaking is consistent with a change in effective collisionality (expressed as [10]: $\nu^*=10^{-14}\ Z_{eff}.R.n_e/T_e^2$) between these two configurations.

TRANSP [11] has been run interpretatively for all three cases. The results show a lower ion thermal transport coefficient for the corner case than the other two by typically a factor of 2 to 3 in the confinement region ($0.4<r/a<0.7$). The thermal ion transport coefficient calculations with TRANSP are therefore also consistent with the observations of global energy confinement.

The observations of the kinetic profiles for the three different divertor configurations suggest that the plasma edge and/or divertor conditions impact on the pedestal properties. Pedestal profiles have been studied experimentally using edge charge exchange (for ion temperature and rotation), the HRTS for electron density end temperature [12] and reflectometry (for the edge electron density). The analysis has been made both by ELM averaging over typically 0.5 to 1s of steady state phase and by averaging the pre-ELM values for several ELMs for the same time window. Both analyses give very similar results. In figure 5, pedestal top data averaged over ELMs are shown for the 3 different divertor geometries at different input power and gas rate. The highest pedestal density is found for the horizontal target (where the divertor recycling also dominates, see next section). But the highest ion pedestal pressure is observed for the corner configuration consistently with the core ion temperature as shown in figure 3. The most striking difference comes from the toroidal velocity which is much higher for the corner configuration. The toroidal velocity could play a key role in the edge rotational shear and therefore in the transport quality of the edge barrier. This observation will be further commented in the discussion section. The analyses have also attempted to determine the pedestal characteristics (width and height). There are consistent indications between the HRTS and the edge reflectometry that the density gradient is the strongest for the corner configuration. However, the error bars are quite large on these quantities and more statistical work would be needed before drawing any firm conclusions.

The ELM behaviour is also markedly different for each of the divertor configuration [12] (see figure 1b). In the corner configuration, regular ELMs typically occur with a frequency of 35Hz. The vertical configuration exhibits compound ELMs with a frequency varying from 10 to 100Hz with large excursion of the pedestal temperature (and possibly short transitions back to L-mode) whilst the horizontal configuration has in general high frequency ELMs above 50Hz. Stability calculations made with both MISHKA [13] and ELITE [14] codes show consistently the peeling ballooning limit is different for all three pulses [7]. The vertical configuration has the lowest peeling-ballooning stability limit. The experimental values of edge current and pressure

*See the Appendix of F. Romanelli et al., Proceedings of the 25th IAEA Fusion Energy Conference 2014, Saint Petersburg, Russia

gradient are lying in general close to the stability boundary limit, suggesting that the observed ELMs are consistent with the peeling-ballooning instability for all three cases. There is however differences between the two computations which may arise from sources such as the position of the experimental profiles with respect to the separatrix, the calculation of the edge current (bootstrap model) or the stability criteria used in each model.

4- Characterisation of the neutral recirculation in the divertor and main chamber.

A detailed experimental analysis of the divertor particle recirculation [15] is presented in this section with the objective to identify the potential link between the recycling of neutrals with the confinement and transport observations for all three divertor geometries.

Figure 6a and 6b respectively show the inner and outer divertor Dα from visible spectroscopy emission as a function of the strike-point position for the different fuelling and pumping rates used in the experiment. Typically, the Dα emission increases with fuelling rate and when pumping is decreased (by switching off one of the 2 cryo-pumps toroidally separated by 180deg). With full pumping, the emission levels (Dα) is doubled when the gas fuelling rate is doubled. Reducing pumping by one cryo-pump has also the consequence to increase the Dα emission to similar level than at full pumping with double gas fuelling rate. These observations indicate that the divertor particle source is determined by the balance of gas fuelling and neutral recycling from surfaces on one hand (source) and neutrals pumped (sink) on the other. The amplitude of Dα light emission is found to depend on the strike-points locations, with a drop of a factor of 3 at similar gas injection rate between the horizontal on one hand and the corner and vertical configurations on the other hand, independent of the amount of the input power. The higher pedestal density observed for the horizontal target (fig 3) may also be associated with this high level of recycling. It should be pointed out that the minimum radiation observed for the corner configuration may be due to vignette line of sight into the corner strike point region. The strike point in this particular configuration is not fully viewed by the diagnostic. Thus one cannot draw firm conclusions as to the significance of this minimum. Although not reported on these figures, changing injection location (injection from the main chamber instead of the divertor) has also been tested in this experiment and was found very little impact on the recycling level [16].

The above visible spectroscopy observations are confirmed by the neutral pressure measurements in the sub-divertor which increase by 50% when moving from the horizontal to the vertical configuration. Since the pumped particle flux is proportional to the sub-divertor pressure, more particles are pumped in the vertical configuration leading to a reduction of the effective recycling of particles and this possibly leads to the lower pedestal density observed in this

---

*See the Appendix of F. Romanelli et al., Proceedings of the 25th IAEA Fusion Energy Conference 2014, Saint Petersburg, Russia

divertor configuration. This also could be helped by the proximity of the inner strike to the inner corner which could also participate to the effective pumping, even though the cryo-pump are further from the inner louvre than from the outer.

The data of Fig 6a and 6b are consistent with measurements of the particle flux from Langmuir probes [15]. It can be estimated that the particle flux reaching the target is about 60% lower (peak and integral value) at the outer-strike point in the vertical configuration compared with the horizontal one. However, because of the lack of probes in the outer divertor corner in JET, it is not possible to compare these values with those of the corner configuration.

Bolometry reconstructions of the divertor area for all three divertor configurations also show decreasing radiation intensity (by typically a factor of 3) in the X-point area with increasing major radius of the outer strike point (fig 7). This supports again the observation made with visible spectroscopy that neutral recirculation in the divertor is the lowest for the vertical configuration. Given all the above observations, it appears that there is not an obvious correlation between the neutral recycling or divertor radiation in the divertor with the variation of global energy confinement as shown on figure 2.

In JET, the divertor neutral pressure and density are strongly linked with the main chamber values and it has been already observed in the JET-C that the neutral recirculation in the divertor can impact directly onto the main chamber neutral pressure [17] due to the open geometry of the divertor. By changing the divertor geometry, the leakage of neutrals towards the main chamber could change and then impact on the neutral pressure level in the main chamber.

When warming up one of the 2 cryo-pump (therefore switching off the pumping of one pump) for identical discharges of the same experiments an increase of neutral pressure by a factor ~2 is observed for all three divertor configurations at the toroidal location where the pumping is still active, but a much stronger increase of the neutral pressure at the toroidal location where the pump is switched off is observed (factor of ~4, see figure 8. As already shown on figures 6a and 6b, the recycling flux (from visible spectroscopy) is also increased by a factor 2 typically consistently with the toroidal location of this measurement, i.e. in the same toroidal location as the remaining cold cryo-pump. Figure 2, is showing the impact of lower pumping on normalised confinement and the absolute confinement also is in average 10% lower for the pulses with one of the cryo-pump warm. This test emphasizes that neutrals do impact on global confinement although it is difficult at this stage to assess the role of the strong neutral pressure toroidal asymmetry.

Looking at the variation of the neutral pressure in the main chamber for all divertor configurations (Fig 9), it can be observed that the corner configuration has the lowest main

---

*See the Appendix of F. Romanelli et al., Proceedings of the 25th IAEA Fusion Energy Conference 2014, Saint Petersburg, Russia

chamber pressure in comparison to the horizontal and vertical ones. Doubling the gas rate (in the divertor) typically increases the pressure by the same amount (Fig 8) which emphasizes the connection between the neutral pressure in the divertor and in the main chamber. It is also interesting to note that increasing the input power has the effect of increasing the neutral pressure in the main chamber whilst preserving the same trend. This effect could be associated with the increased Be (and Deuterium) recycling and erosion at higher power as described in [18]. The levels of neutral pressure shown in Fig 9 are also consistent with Dα emission level monitored in the main chamber. Figure 10 presents the total pedestal pressure from kinetic measurements versus the main chamber pressure for the same database of pulses. At a given gas injection and input power, an anti-correlation of the pedestal pressure with the main chamber pressure is observed when the strike point position is varied indicating a possible physical link between the main chamber neutrals and the loss of confinement.

Past experiment with the carbon wall had also reported the impact of neutral in the main chamber on confinement. With the JET-C, it was pointed out that the separatrix density could be the source of the confinement degradation [19]. Also, more recently, the loss of confinement in high triangularity hybrid scenario in JET-C has been correlated with an increase of the neutral pressure and recycling in the main chamber [5, 20]. Although the causality between main chamber and confinement is not formally demonstrated here, the new ILW data evidence points towards a similar neutral effect on energy confinement as for the previous experiments with the C-wall. It is unlikely that the difference in confinement observed for one given divertor geometry between the JET-C and the JET-ILW (see Fig 2), can be attributed to neutrals since the neutral circulation between the two wall material had no reason to change. On the other hand, the above evidence suggesting that the difference observed between divertor configuration are connected with neutral pressure in the main chamber.

.

5- Discussion

In this section, some possible physics mechanisms are reviewed with the attempt to identify the mechanism which could explain the loss of pedestal energy confinement in these experiments with different divertor geometry.

Modelling of the discharges with different divertor configuration has been carried out using the EDGE2D-EIREINE [22] and SOLEDGE2D-EIREINE [23] codes with the objective to investigate the interaction of the neutrals with the pedestals. In general, these calculations have used the equilibrium and the total heating power as input with no impurities thus concentrating on the deuterium specie. Inside the separatrix, the cross-field heat and particle transport is adjusted

*See the Appendix of F. Romanelli et al., Proceedings of the 25th IAEA Fusion Energy Conference 2014, Saint Petersburg, Russia

to reproduce the measured pedestal density and temperature. The first possible loss channel that has been examined is the ion energy losses on edge neutrals through charge exchange processes. In the two extreme configuration (horizontal and vertical outer divertor strike point), the last closed flux surface comes close to the divertor baffles (see fig 1). In addition, in the main chamber, the proximity to the wall may also induce charge exchange losses through higher level of neutral. The calculations with SOLEDGE2D (fig 11) [15] are showing that the charge exchange losses are dominant in the main chamber. This is consistent with the neutral pressure measurements in the mid-plane. However, in all cases the order of magnitude of the energy loss channel is too small to explain the observed fall in energy confinement in the experiment. The divertor geometry does lead to a variation of the losses compatible with the confinement variation (there is a minimum loss for the corner configuration) but the losses do not exceed 1MW out of 15MW crossing the separatrix. This is also confirmed by EDGE2D-EIREINE simulations [24] showing that pedestal charge exchange losses are typically less than 5% of the power crossing the separatrix (Psep). Consequently, the neutral power losses inside the confined region of the plasma are generally small and unlikely to explain the observed reduction in energy confinement. This is suggesting that the responsible mechanism is probably implicit and may be related to a modified radial transport in the pedestal due to changes in the divertor and SOL.

Another possible loss channel resides in the observation that the corner configuration shows a much higher toroidal velocity (fig 5) than the other two configurations. Here, we examine the hypothesis that neutral recycling could modify the ion flow in the vicinity of the edge barrier shear (ETB) layer and degrades the ETB as a result. The force balance equation for the main ion can be written as: $E_r = \frac{T_i}{en_i}\frac{\partial n_i}{dr} + (1-\kappa)\frac{\partial T_i}{\partial r} + V_T B_P$, where the poloidal velocity has been replaced by its neoclassical value, κ~0.5-1.5 depending on the collisionality regime and B_P the local poloidal field. From figure 3, the gradient of the ETB can be inferred and one comes to the conclusion that the density gradient terms (first term) dominate E_r by a factor 2 to 5 over the last two terms of the equation above. This suggests that edge particle transport could have a strong impact on the rotational shear at the edge and may impact on the strength of the ETB. Experimentally at JET [25], it has been observed in the JET-C that the angular momentum can be considerably affected with a significant lowering of the thermal Mach number at the edge when the neutral pressure is increased. Therefore neutrals may potentially participate to the momentum loss by friction with the ions and change the ETB strength.

To test this, an external force inside the separatrix has been adjusted in the momentum balance in EDGE2D-EIREINE such that flow velocities would be close to the sound speed. The

---

*See the Appendix of F. Romanelli et al., Proceedings of the 25th IAEA Fusion Energy Conference 2014, Saint Petersburg, Russia

neutral friction is calculated inside the separatrix and indicates much lower amplitude than the momentum transport to the SOL. This indicates that the viscous transport of momentum to the scrape-off layer can dominate over the impact of neutral friction on the rotation.

The effect of the neutrals on the ion flow has also been examined theoretically [26]. It was suggested that if neutrals are not affecting the ion flow they could, on the other hand, strongly modify the electrostatic potential just inside the separatrix either through their large viscosity [27] or through charge separation when different type of neutrals are present [28]. Tungsten impurities eroded from the divertor could also modify the SOL characteristics by atomic physics processes as shown in [29]. The SOL composition of neutrals (carbon in JET-C, Be and W in JET-ILW) may thus modify the charge separation and therefore the electrostatic potential. Therefore neutrals may be responsible for significant radial variation of the electric field and thereby be responsible for change in the ExB shear. However, so far, only the upstream density could be measured using the Lithium beam and the reflectometer diagnostics. But no temperature measurements could be made. It is therefore challenging to fully characterise the changes at the foot of the ETB. These measurements can be reliably made only for the horizontal divertor configuration. For the other divertor configurations the diagnostic viewing lines does not cover the area where the outer strike point is located making any comparison difficult to interpret.

6- Conclusions

H-mode experiments at JET with the ITER-like wall have demonstrated that changes in divertor strike point position are correlated with strong modification of the global energy confinement. Typically the normalised energy confinement factor can vary from 0.7 to 0.95 and is a maximum when the outer strike is close to (or inside) the pumping throat. The IPB98y2 confinement scaling law predicts an identical confinement time for all three configuration in contradiction with these observations.

The impact on energy confinement is observable both on the pedestal confinement and core normalised gradients. The vertical divertor configuration shows a much lower pedestal density and pressure. The corner configuration shows an increased core density gradient length and ion pressure indicating a better ion confinement than the two other divertor configurations.

Pedestal ion pressure and toroidal velocity is also stronger than in the other configuration and there are indications that the density gradient of the ETB is also larger. This suggests that the corner configuration has a smaller pedestal transport than the other two configurations.

The study of neutral re-circulation indicates that the neutral recycling in the divertor is not correlated with the confinement. On the other hand, the neutral pressure in the main chamber

---

*See the Appendix of F. Romanelli et al., Proceedings of the 25th IAEA Fusion Energy Conference 2014, Saint Petersburg, Russia

varies inversely with the energy confinement and a correlation between the pedestal total pressure and the neutral pressure in the main chamber can be established although formally the causal link has not yet been demonstrated. This is in line with past observations made in the JET-C.

So far, it does not appear that the energy losses on edge neutrals induced in the pedestal by charge exchange can explain the loss of pedestal confinement. Computed charge exchange losses with edge codes amounts to less than 5% of the power going through the separatrix over both the divertor and main chamber area. Momentum losses are another potential candidate but preliminary calculation does not seem to confirm this hypothesis despite contradicting past experimental results in the JET-C. However, it may be that the neutrals can also affect directly the edge electric potential as suggested in [22] and therefore the ExB shear inside the separatrix that could determine the edge barrier quality. More experimental and modelling work is necessary here to infirm or confirm this hypothesis.

The performance achieved in both baseline and hybrid scenario described in this paper emphasizes the operational importance of pumping in the main chamber with the JET-ILW. Even though these experiments are not representative of the divertor conditions expected in ITER (i.e. semi-detachment), since ITER has limited pumping capabilities (~150m^3/s for a volume of ~1000m^3), it is essential to understand the underlying physics that governs the interaction between the neutrals in the main chamber and the pedestal leading to changes in pedestal and core energy confinement with a metallic wall environment.

Acknowledgement

This work was carried out within the framework of EUROfusion Consortium and has received funding from the Euratom research and training programme 2014-2018 under grant agreement No633053. The views and opinions expressed herein do not necessarily reflect those of the European Commission".

References

[1]: G. F. Matthews et al., Physica Scripta 2011 (T145), 014001

[2]: E. Joffrin et al., Nucl. Fusion (2014) 54 013011.

[3]: M. Brix et al., Rev Sci Instrum. (2008) 79 (10):10F325.

[4] : I. Nunes et al., 25th Fusion Energy Conference, Saint-Petersburg, 2014, EX/9-2

[5] : C. Challis et al., Nuc. Fusion 55 (2015) 053031

[6]: M. Beurskens et al., Nuc Fusion 48 (2008) 095004

[7]: C. Maggi et al., to be published in Nuc. Fusion 2015

*See the Appendix of F. Romanelli et al., Proceedings of the 25th IAEA Fusion Energy Conference 2014, Saint Petersburg, Russia

[8]: ITER physics basis, 1999, Nuc. Fus. 39 (1999) 2175

[9] : A. Kallenbach et al., 2002 Nuc. Fusion 42 (2002), 1184.

[10] : M. Maslov et al., Nuc Fusion 49 (2009), 075037

[11]: Goldston R. J. et al, J. Comput. Phys. 43 (1981), 61

[12]: L. Frassinetti et al. 41st European Physical Society Conference (Berlin, Germany 2014), P1-030

[13]: A.B. Mikhailovski et al., Plasma Phys. Report, 23 (1997) 844

[14]: Wilson H.R., Phys. Plasmas 9 (2002) 1277

[15]: P. Tamain et al. 21st International Conference on Plasma surface Interaction, Kanazawa, Japan, 2014, O33

[16]: M. Groth et al., Nucl Fusion 53 (2013) 093016

[17]: A. Loarte et al., Plasma Phys. Control Fusion 43 (2001) R183-R224

[18]: S. Brezinsek, 21st International Conference on Plasma surface Interaction, Kanazawa, Japan, 2014, R2

[19]: L. Horton et al. Nuc. Fusion 39 (1999) 1

[20]: E. Joffrin et al. 41st European Physical Society Conference, (Berlin,Germany, 2014), O4.125

[21]: A. Kallenbach et al., Nucl. Fusion 43 (2003) 573

[22]: D. Reiter, Jour. Nucl. Mater. 196 - 198 (1992) 80

[23]: H. Bufferand et al., J. Nucl. Mat. 2013

[24]: A. Jarvinen et al., this Fusion Energy Conference, 2014, TH/P5-34

[25]: T. Versloot et al. Plasma Phys. Control. Fusion 53 (2011) 065017

[26]: T. Fülop et al., Physics of Plasma, 8 (2002) 5214

[27]: P. Catto, et al., Phys. Plasma 5, 3961 (1998)

[28] : M. Shoucri et al., Computer Physics Communications 07/2001; 137(3):396-404.

[23]: C. Giroud et al., Nuc. Fusion 53 (2013) 113025

*See the Appendix of F. Romanelli et al., Proceedings of the 25th IAEA Fusion Energy Conference 2014, Saint Petersburg, Russia

Figure captions

Fig 1a*: Divertor geometry used in JET (horizontal=blue; corner=green; vertical=red). The cryogenic pump is also pictured in black bold traces. The broken arrow indicates the origin of the R coordinates used for the outer strike point position in the next figures. The black dot indicates the point of gas injection used in this experiment. Note that this injection is always in the private flux area independently from the divertor geometry.*

Fig 1b: *comparison of the discharges with the three different divertor configuration pictured in figure 1a. These discharges have all Ip=2.5MA, B_T=2.7T, the same input power, and the same gas injection inside the private area of the divertor. The discharge with the strike point in the corner (green) shows the highest confinement. Note also the differences in ELM frequency and amplitude.*

Fig 2*: Normalised confinement factor as function of the outer strike point positions for discharge with identical, volume plasma current (Ip=2.5MA), magnetic field (B_T=2.7T) at different injected power (15 & 22MW), gas injection rate and divertor pumping (1/2 cryo pump is switched off for the open green circles). Grey dots are data for equivalent JET-C discharges for comparison.*

Fig 3: *Electron density, temperature and pressure (from Thomson scattering diagnostic) and ion temperature (from charge exchange diagnostic) and ion pressure for the three divertor geometry cases. The data are taken during the high power phase (23MW) and averaged over 0.5s around t=11.5s (see figure 2).*

Fig 4: *Total pedestal pressure (o) and core gradient lengths at $0.4<\rho<0.7$ (-). Density gradient length (△) varies like the pedestal pressure (o) by almost a factor of 2.*

Fig 5*: pedestal density and electron pressure from the Thomson scattering diagnostic and toroidal rotation and ion pedestal pressure from the edge charge exchange diagnostic for the 3 different divertor geometries characterized by the outer strike position from the centre of the divertor (see figure 1a). The data are averaged over over the ELM activity for 0.5s during the low power phase (15MW) and the high power phase (23MW) for the different situation of gas injection rate.*

Fig 6a: *Variation of the recycling emission in the inner divertor for the three divertor configurations for different gas injection rate and with ½ of the cryo.*

Fig 6b: *Variation of the recycling emission in the outer divertor for the three divertor configurations for different gas injection rate and with ½ of the cryo.*

Fig 7: *Radiation reconstruction from the bolometry cameras for the three divertor configuration (horizontal – corner – vertical) in the high power phase (23MW). Note that the emission is the strongest for horizontal target configuration and the lowest for the vertical one.*

Fig 8: *Effect of the pumping on the main chamber neutral pressure for all three divertor geometry. Open symbols are the main chamber pressure measurements with both cryo-pumps cold (i.e. pumping) and filled symbols with one of the 2 cryopump warm (i.e. not pumping). Diamonds are the neutral measurements made at the toroidal location close to the pump that stays cold all the time and squares are measurements close to the cryo-pump which is switched off. Note the strong neutral pressure toroidal asymmetry when one of the pump is warmed-up.*

---

*See the Appendix of F. Romanelli et al., Proceedings of the 25th IAEA Fusion Energy Conference 2014, Saint Petersburg, Russia

The neutral pressure is increased by a factor of ~4 closed to the warm pump and a factor of 2 close to the cold (pumping) pump.

Fig 9: *Variation of the main chamber pressure measured by pressure gauges for the three divertor configurations for different gas injection rate and input power.*

Fig 10: *Correlation of the total pedestal pressure with the neutral pressure measured in the main chamber for different gas injection rate and input power when the strike point position is varied in each case.*

Fig 11: *Modelling with the SOLEDGE-EIREINE code for all three divertor geometry. Recycling areas are present on the divertor baffles but is actually dominant in the main chamber on the outboard side. In all cases the charge exchange losses are very small (<1MW) and cannot explain the differences observed on the global confinement between the 3 divertor shapes.*

*See the Appendix of F. Romanelli et al., Proceedings of the 25th IAEA Fusion Energy Conference 2014, Saint Petersburg, Russia

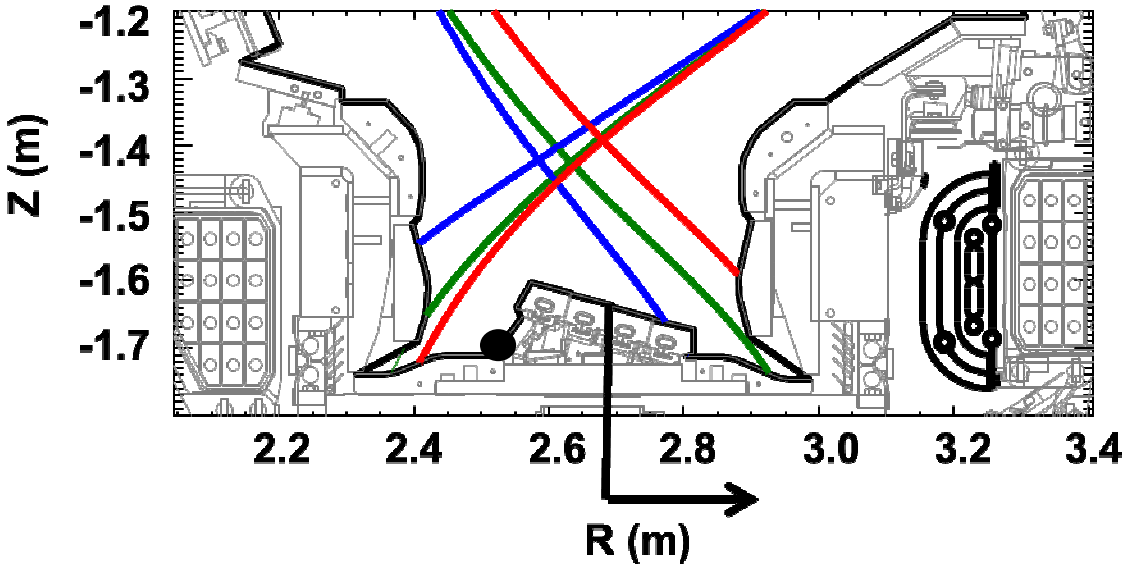

Figure 1a

*See the Appendix of F. Romanelli et al., Proceedings of the 25th IAEA Fusion Energy Conference 2014, Saint Petersburg, Russia

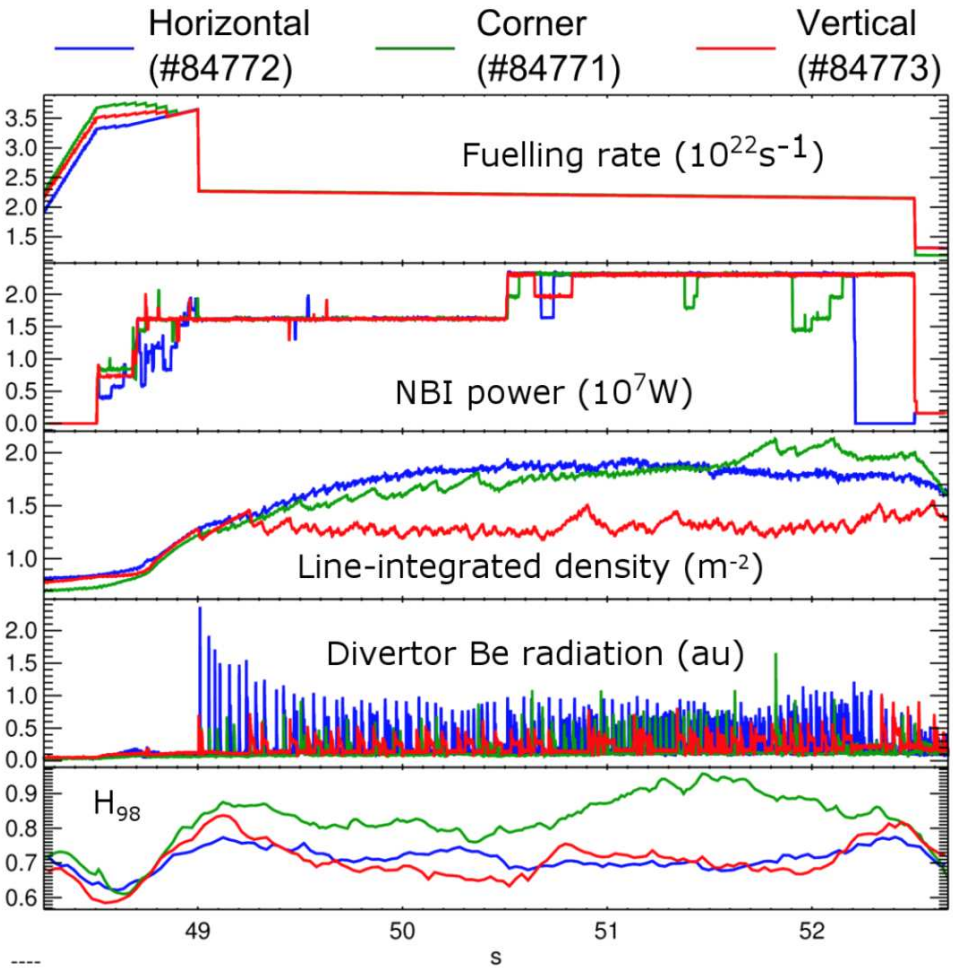

Figure 1b

*See the Appendix of F. Romanelli et al., Proceedings of the 25th IAEA Fusion Energy Conference 2014, Saint Petersburg, Russia

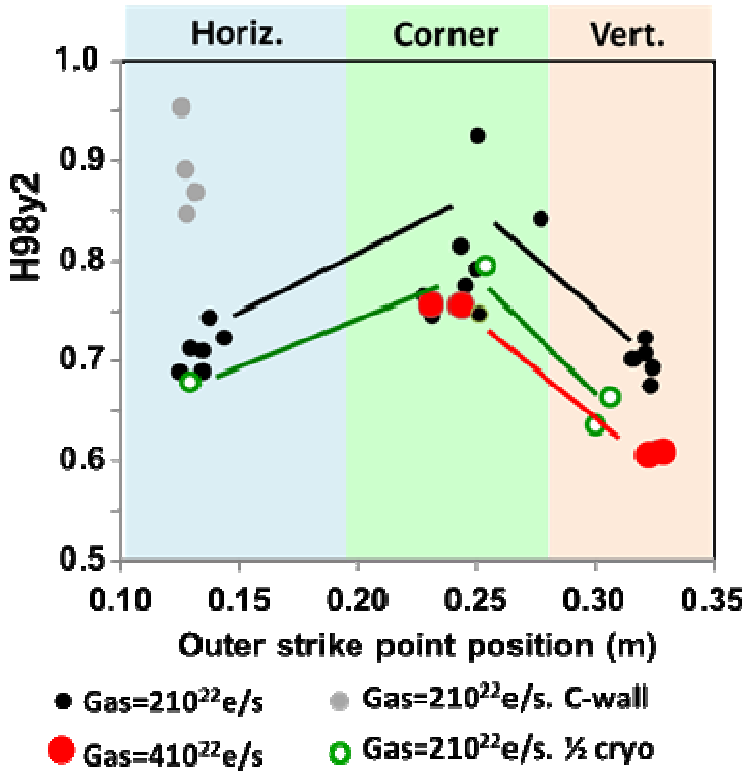

Figure 2

*See the Appendix of F. Romanelli et al., Proceedings of the 25th IAEA Fusion Energy Conference 2014, Saint Petersburg, Russia

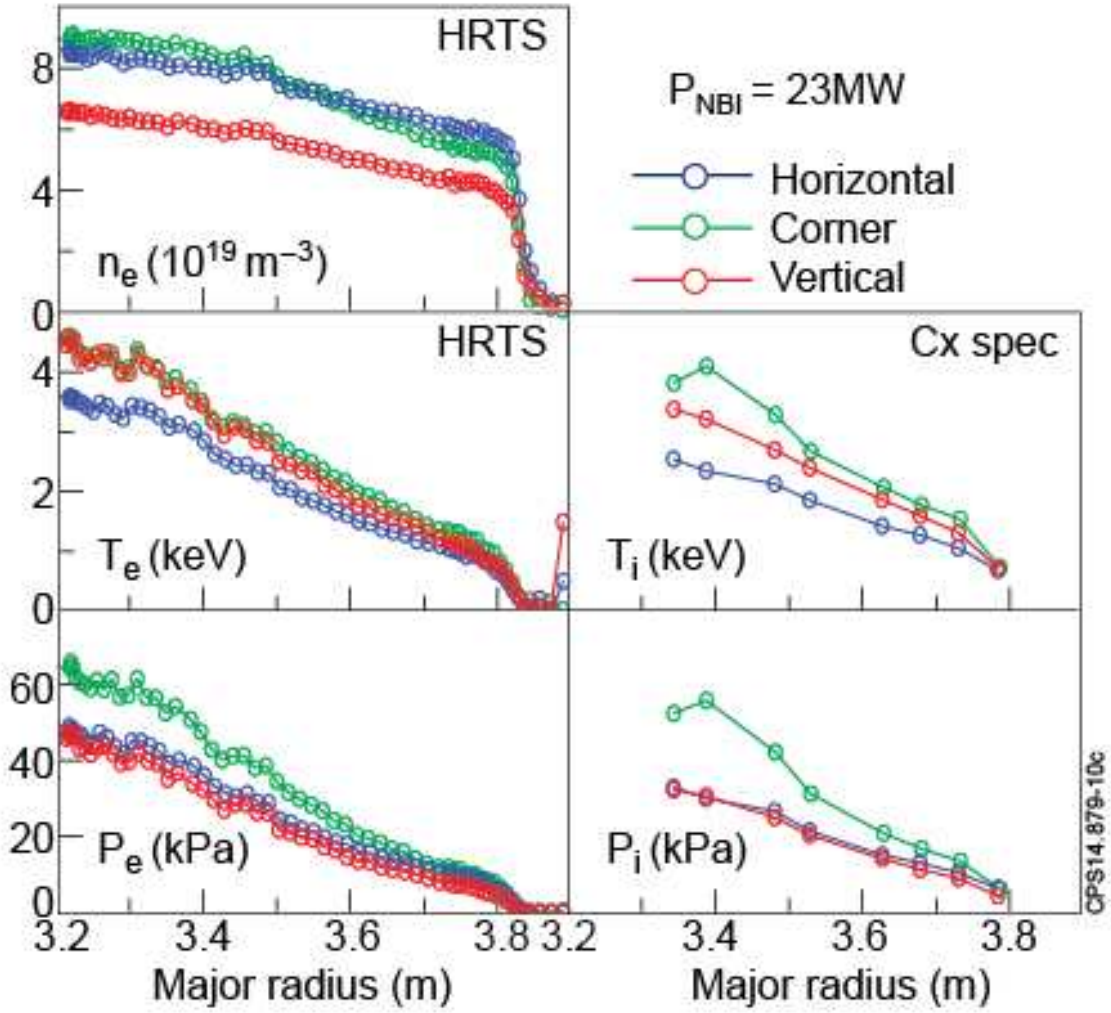

Figure 3

*See the Appendix of F. Romanelli et al., Proceedings of the 25th IAEA Fusion Energy Conference 2014, Saint Petersburg, Russia

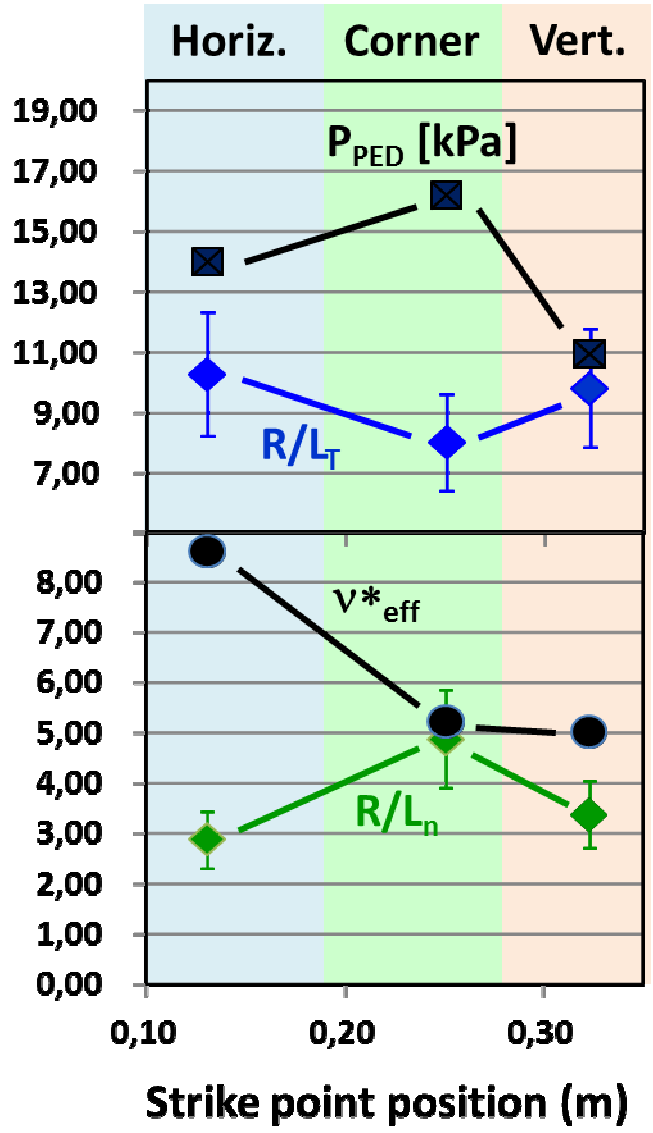

Figure 4

*See the Appendix of F. Romanelli et al., Proceedings of the 25th IAEA Fusion Energy Conference 2014, Saint Petersburg, Russia

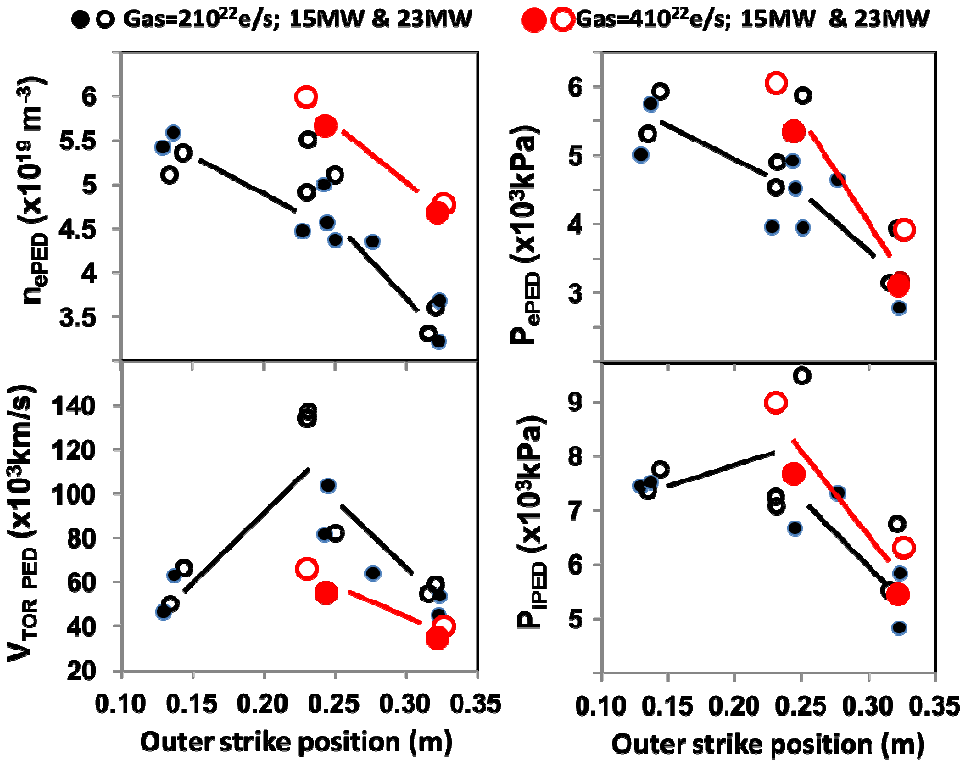

Figure 5

*See the Appendix of F. Romanelli et al., Proceedings of the 25th IAEA Fusion Energy Conference 2014, Saint Petersburg, Russia

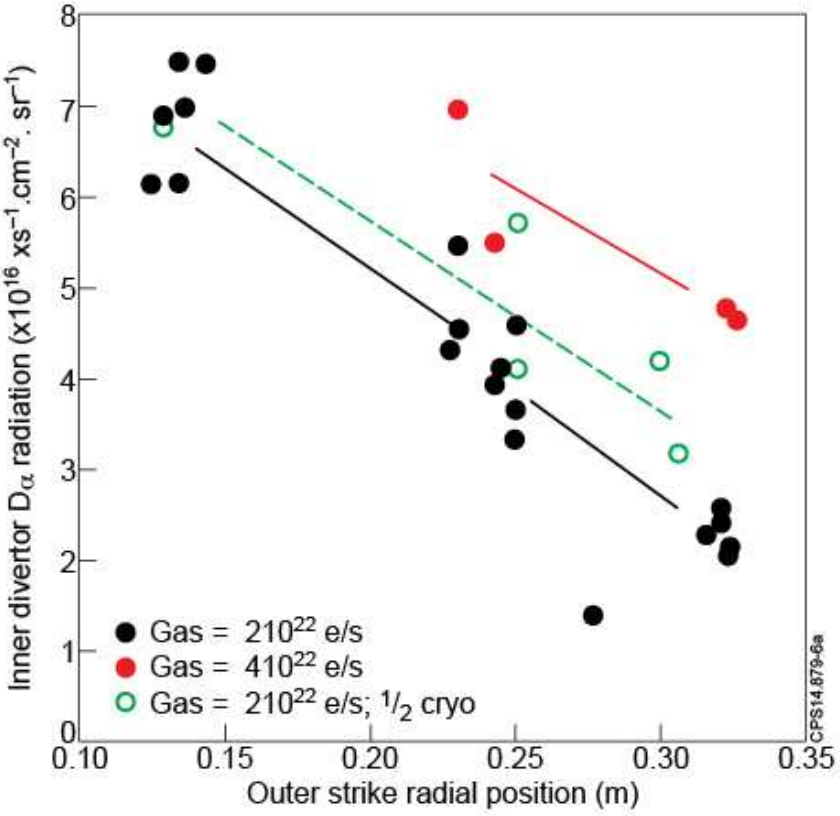

Figure 6a

*See the Appendix of F. Romanelli et al., Proceedings of the 25th IAEA Fusion Energy Conference 2014, Saint Petersburg, Russia

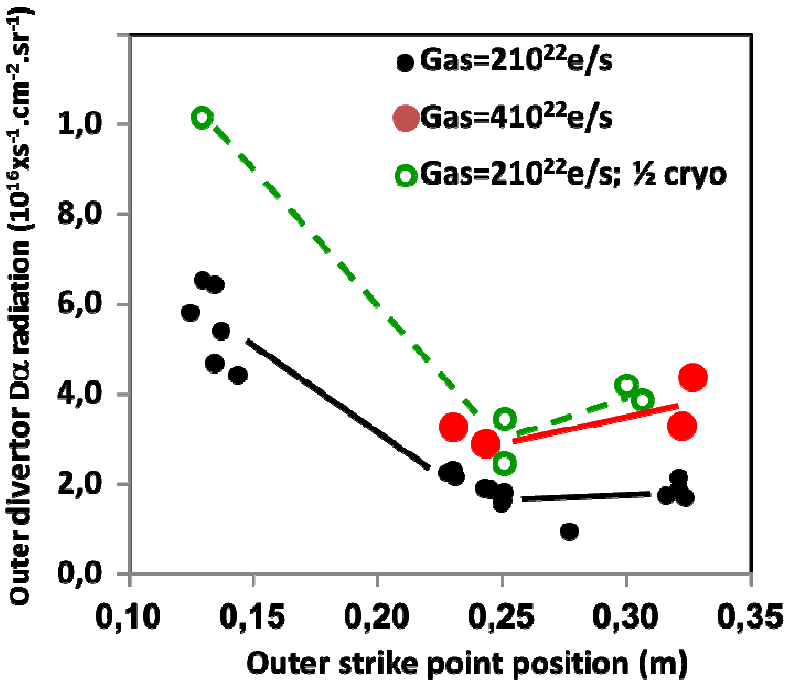

Figure 6b

*See the Appendix of F. Romanelli et al., Proceedings of the 25th IAEA Fusion Energy Conference 2014, Saint Petersburg, Russia

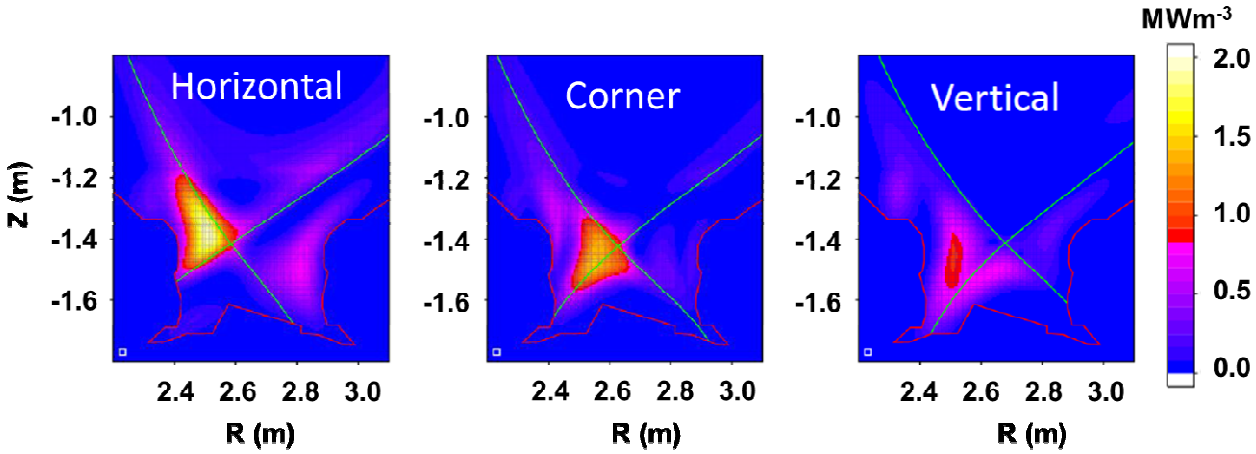

Figure 7

*See the Appendix of F. Romanelli et al., Proceedings of the 25th IAEA Fusion Energy Conference 2014, Saint Petersburg, Russia

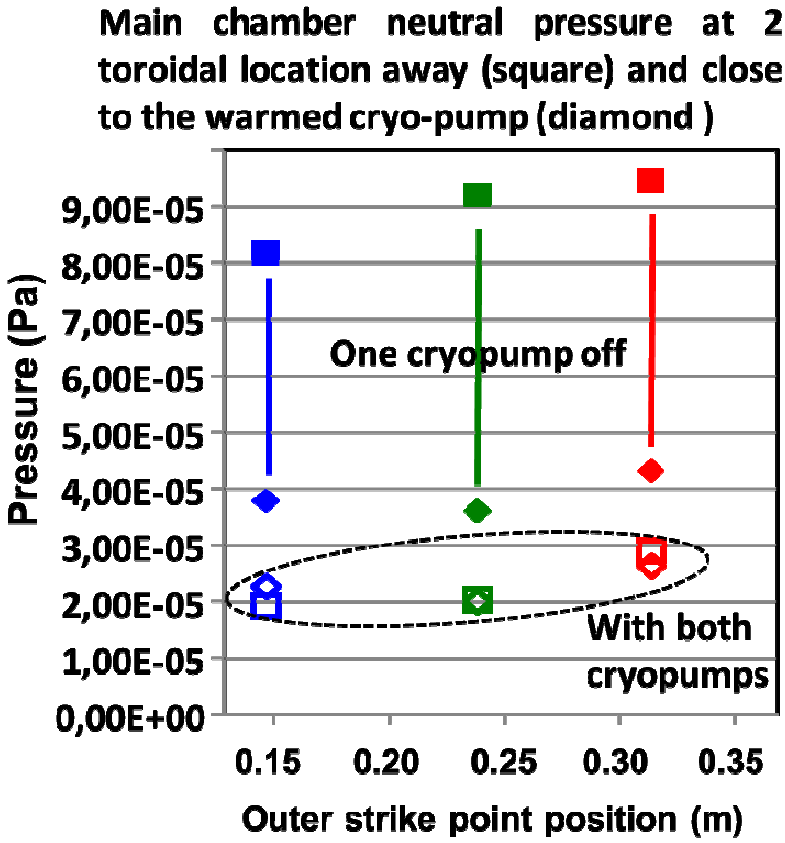

Figure 8

*See the Appendix of F. Romanelli et al., Proceedings of the 25th IAEA Fusion Energy Conference 2014, Saint Petersburg, Russia

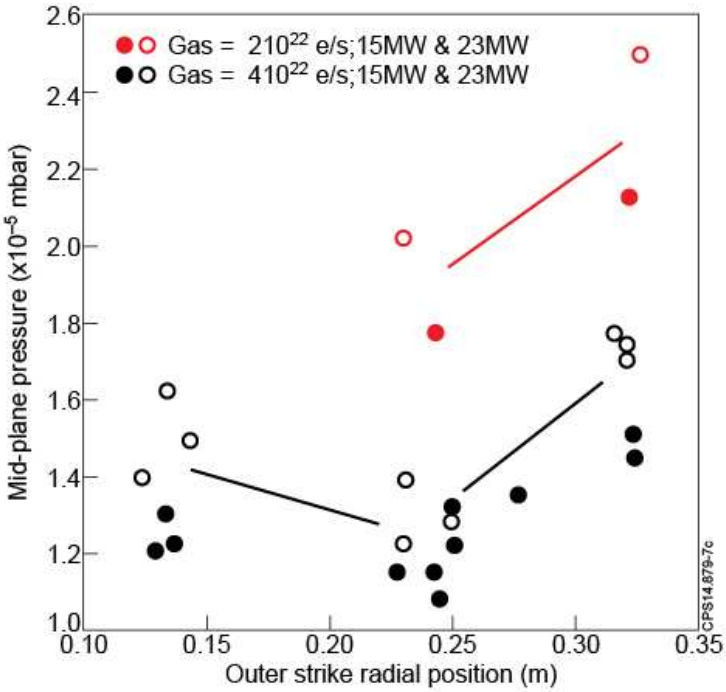

Figure 9

*See the Appendix of F. Romanelli et al., Proceedings of the 25th IAEA Fusion Energy Conference 2014, Saint Petersburg, Russia

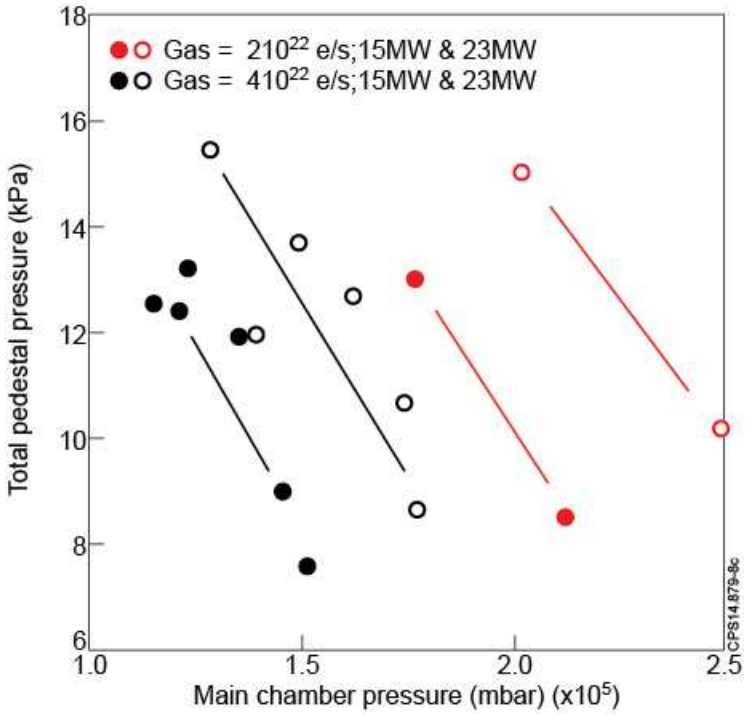

Figure 10

*See the Appendix of F. Romanelli et al., Proceedings of the 25th IAEA Fusion Energy Conference 2014, Saint Petersburg, Russia

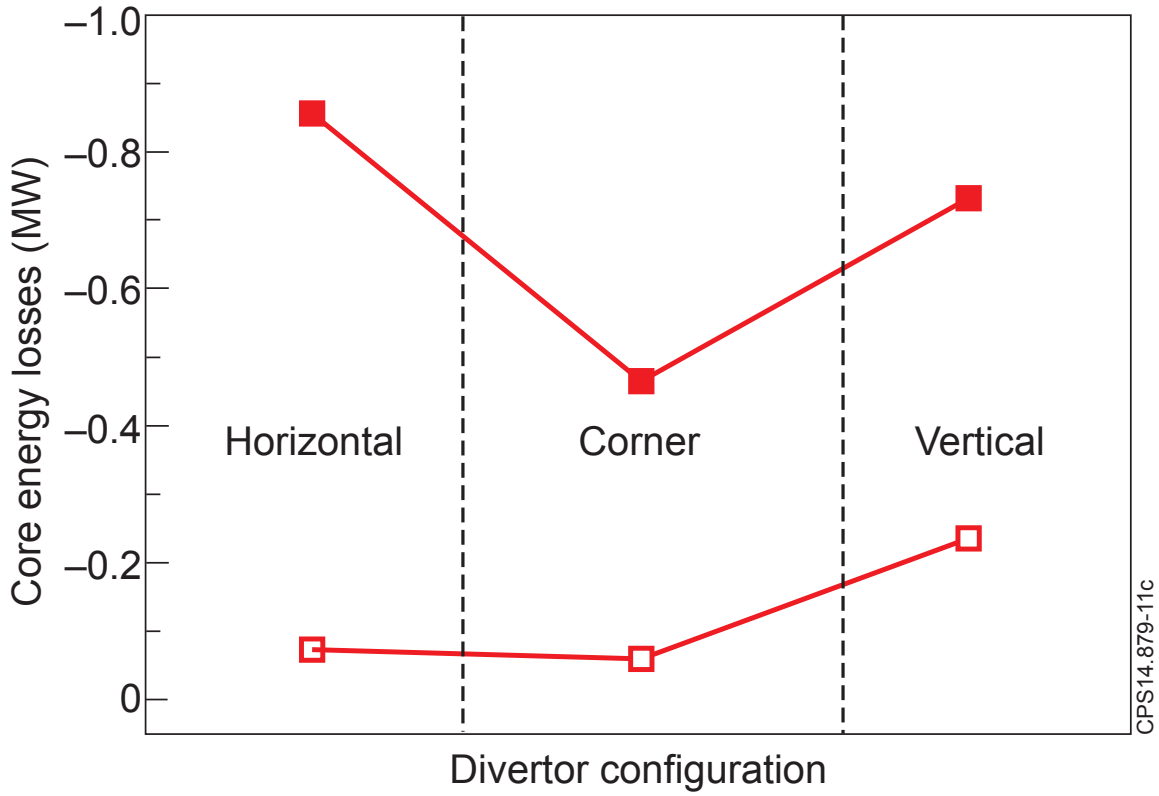

Figure 11

*See the Appendix of F. Romanelli et al., Proceedings of the 25th IAEA Fusion Energy Conference 2014, Saint Petersburg, Russia